

Numerical simulation of the dispersion of contaminants by a characteristic-based method with applications to the Ebro delta and the Huelva estuary

Jordi BLASCO¹, Arnel GERMAN², Manuel ESPINO²,
M. Augusto MAIDANA²

¹ Dept. de Matemàtica Aplicada I, Univ. Politècnica de Catalunya
Campus Sud, Edifici H, Avgda. Diagonal 647, 08028 Barcelona

² Lab. de Ingeniería Marítima, Univ. Politècnica de Catalunya
Campus Nord, Edifici D1, c/Gran Capità s/n, 08034 Barcelona

jorge.blasco@upc.edu, arnel.german@upc.edu,
manuel.espino@upc.edu, augusto.maidana@upc.edu

Abstract

In this paper we consider an explicit, characteristic-based method for the numerical simulation of the dispersion of contaminants in a fluid medium. A quasi-3D formulation is employed for the spatial approximation. Two real-life applications of the model developed are presented: the dispersion of the plume of the Ebro river and the thermal outflow of power plants in the Huelva estuary.

1 Introduction

Among several other sources of pollution in the sea, contaminant spills, underwater sewers, thermal plumes and, more recently, saline plumes can be cited. Dispersion of these pollutants in the fluid receptors is the only way to reduce the degree of concentration traditionally relied on. The increase in human activity requires higher standards of water management, and numerical models provide an efficient tool to simulate contaminant dispersion.

The differential model generally accepted to govern transport phenomena is the transient convection-diffusion-reaction equation (see [6]). Its numerical solution, however, may lead to the well-known node-to-node oscillations (see [1]) if standard approximations are used. Several stabilization techniques have been proposed in order to avoid those numerical difficulties (see [1], [2], [3] and [5], among several others). Many of these formulations depend on arbitrary algorithmic parameters, which need some tuning in order to achieve the best accuracy possible. An explicit, characteristic-based method ([3], [10]) is employed in our model; in this scheme, which is parameter-free, some stabilizing terms are introduced through a Taylor expansion of the solution along the characteristic curves.

On the other hand, most existing codes for the numerical simulation of pollutant transport are based on two-dimensional formulations; 2D-H schemes, for instance, employ vertically averaged equations. Taking into account the large computational effort required for accurate fully three-dimensional transient simulations, we opted for a quasi-3D approximation ([8], [9]), in which the horizontal and vertical variables are discretized in a different way.

The model just described has been so far applied to two real-life situations. In the first case, the dispersion of the plume of the Ebro river in the Mediterranean sea was analyzed, while in the second case the dispersion of the thermal outflow of some power plants in the Huelva estuary was studied.

The outline of the paper is as follows: in Section 2 we state the mathematical problem to solve. The temporal and spatial discretizations used are presented in Sections 3 and 4, respectively, while in Section 5 the numerical results obtained in the two applications considered are presented. Finally, some conclusions are drawn.

2 The convection-diffusion-reaction equation

We recall here the transient convection-diffusion-reaction equation as a model for contaminant dispersion in a fluid medium. Given a three-dimensional domain Ω , a divergence-free velocity field $\mathbf{u} = (u_1, u_2, u_3)$ defined on Ω and a final time $T > 0$, the problem consists in finding a scalar function $\phi: \Omega \times [0, T] \rightarrow \mathbb{R}$, representing the concentration of contaminant, such that:

$$\frac{\partial \phi}{\partial t} + \frac{\partial F_i}{\partial x_i} + \frac{\partial G_i}{\partial x_i} + R + S\phi = 0 \quad (1)$$

where repeated indices imply summation and the following notation is used: $(x_1, x_2, x_3) = (x, y, z)$ are the spatial coordinates; $t \in (0, T)$ is the time variable, $F_i = u_i \phi$ are the convective fluxes; $G_i = -k_i(\partial \phi / \partial x_i)$ are the diffusive fluxes, with $(k_1, k_2, k_3) = (k_H, k_H, k_V)$ the two horizontal and vertical turbulent diffusivity coefficients, respectively; R is a source or a sink term and S represents the sedimentation velocity.

Boundary conditions have to be supplied to equation (1). Zero normal flux is imposed on the surface (denoted hereafter by \mathcal{S}), the bottom and outflow lateral boundaries, whereas prescribed concentration is considered at inflow boundaries:

$$\begin{aligned} \text{Lateral boundaries :} \quad & \phi = \phi^* \quad \text{if } u_1 n_1 + u_2 n_2 < 0 \\ & k_H \frac{\partial \phi}{\partial x} n_1 + k_H \frac{\partial \phi}{\partial y} n_2 = 0 \quad \text{if } u_1 n_1 + u_2 n_2 \geq 0 \\ \text{Surface and bottom :} \quad & k_V \frac{\partial \phi}{\partial z} = 0 \quad \text{if } z = 0 \text{ or } z = -\mathcal{H} \end{aligned}$$

where $\mathbf{n} = (n_1, n_2, n_3)$ is the unit outward normal vector to the boundary of Ω and $\mathcal{H}(x, y)$ is the bottom depth.

An initial condition is also required:

$$\phi(\mathbf{x}, 0) = \phi_0(\mathbf{x})$$

3 Numerical solution

It is well known that the numerical solution of advection-diffusion problems like (1) may give rise to unphysical oscillations of the numerical solution (see [1]). Several ways have been developed to avoid those oscillations, commonly referred to as stabilization techniques. To name a few: the Streamline-Upwind-Petrov-Galerkin or SUPG formulation ([1]), the Galerkin-Least-Squares or GLS method ([5]), the Taylor-Galerkin method ([2]) and the Characteristic-Galerkin method ([3]). One drawback of some of these techniques is that their efficiency relies on the selection of the value of algorithmic parameters which have to be tuned on test cases. We opted to use an explicit, Characteristic-Galerkin approximation which is parameter free, has the desired stabilization properties and the simplicity of explicit schemes. We describe this method as follows.

3.1 Temporal approximation

The method of characteristics is based on the consideration of the characteristic curves X_i such that:

$$\frac{dX_i}{dt} = u_i(X_i(t), t)$$

If equation (1) is written in the coordinate system given by X_i , the convective terms disappear, since the reference itself moves with the flow:

$$\frac{\partial \phi}{\partial t} + \frac{\partial G_i}{\partial X_i} + R + S\phi = 0 \quad (2)$$

The notation x_i will be used again for X_i in what follows for simplicity of exposition. An explicit forward-Euler temporal approximation is then introduced in (2). Given a time step size $\Delta t > 0$, an approximation ϕ^{n+1} to ϕ at time $t_{n+1} = (n+1)\Delta t$ is calculated at each point $\mathbf{x} \in \Omega$ from known values at time $t_n = n\Delta t$ by:

$$\frac{\phi^{n+1}(\mathbf{x}) - \phi^n(\mathbf{x} - \boldsymbol{\delta})}{\Delta t} = - \left(\widetilde{\frac{\partial G_i}{\partial x_i}} + \widetilde{(R + S\phi)} \right)^n \quad (3)$$

Variables with a superscript n are evaluated at time t_n and $(\mathbf{x} - \boldsymbol{\delta})$ is the point at time $t = t_n$ along the characteristic which is located at \mathbf{x} at time $t = t_{n+1}$. The right-hand side terms are evaluated at some point along the characteristic to be determined later on.

Using a second-order Taylor expansion of the solution around \mathbf{x} , gives:

$$\phi^n(\mathbf{x} - \boldsymbol{\delta}) \simeq \phi^n(\mathbf{x}) - \boldsymbol{\delta}^t \cdot \nabla \phi(\mathbf{x}) + \frac{1}{2} \boldsymbol{\delta}^t \nabla (\nabla^t \phi(\mathbf{x})) \boldsymbol{\delta}$$

where $\nabla = (\frac{\partial}{\partial x}, \frac{\partial}{\partial y}, \frac{\partial}{\partial z})^t$. The following approximations are then considered:

$$\begin{aligned}\delta_i &\simeq \tilde{u}_i \Delta t \\ \tilde{u}_i &\simeq u_i - \frac{\Delta t}{2} u_j \frac{\partial u_i}{\partial x_j} \\ \widetilde{\left(\frac{\partial G_i}{\partial x_i}\right)}^n &\simeq \left(\frac{\partial G_i}{\partial x_i}\right)^n \\ \widetilde{(R + S\phi)}^n &\simeq (R + S\phi)^n - \frac{1}{2} \delta^t \cdot \nabla (R + S\phi)^n\end{aligned}$$

Substituting these expressions in (3), rearranging terms, taking into account the incompressibility of the fluid and neglecting higher order terms in Δt leads to the following explicit scheme:

$$\begin{aligned}\phi^{n+1} &= \phi^n - \Delta t \left(u_i^n \frac{\partial \phi^n}{\partial x_i} - \frac{\partial}{\partial x_i} (k_i^n \frac{\partial \phi^n}{\partial x_i}) + R^n + S^n \phi^n \right) \\ &\quad + \frac{\Delta t^2}{2} \left(u_j^n \frac{\partial}{\partial x_j} (u_i^n \frac{\partial \phi^n}{\partial x_i} + R^n + S^n \phi^n) \right)\end{aligned}\quad (4)$$

It can be readily observed that additional terms are added to the standard forward Euler scheme which introduce a streamline upwind effect that stabilizes the numerical solution.

The simplicity and efficiency of an explicit scheme like (4) is always obtained at the expense of conditional stability. The value of the time step is limited by a condition on the element Courant number $C^e = \frac{u^e \Delta t}{h^e}$, where u^e is a characteristic value of the velocity at element e and h^e is its size, so that:

$$C^e \leq \sqrt{\frac{1}{\text{Pe}^2} + \frac{1}{3}} - \frac{1}{\text{Pe}} \quad (5)$$

In (5), $\text{Pe} = \frac{u^e h^e}{2k^e}$ is the element Peclet number, k^e being the maximum coefficient of diffusivity on the element. The stability restriction (5) has to be respected on all elements.

3.2 Quasi-3D spatial approximation

The semidiscrete problem (4) is now further discretized in space. In order to avoid the limitations of two-dimensional approximations, like vertically averaged formulations, and to reduce the computational effort of fully three-dimensional discretizations, a quasi-3D approximation is employed (see [8], [9]). That is to say, the vertical and horizontal variations of the solution are approximated separately, and while a spectral method is employed for the vertical variable, a finite element method is used for the horizontal discretization.

3.2.1 Vertical approximation

The σ -coordinate formulation is a useful tool which allows to handle the problem with a normalized vertical coordinate ranging from 0 at the bottom to 1 at the surface irrespective of the bottom depth. The adequate change of variables is given by:

$$\sigma = \frac{z + \mathcal{H}}{\mathcal{H} + \eta}$$

where $\eta(x, y)$ is the elevation of the free-surface. The solution is then expressed as a linear combination of some basis functions M_k , which are eigenfunctions of a certain differential operator, with coefficients depending on x and y :

$$\phi^{n+1}(x, y, \sigma) = M_k(\sigma) \phi_k^{n+1}(x, y)$$

Using the Galerkin method of weighted residuals in (4), a system of equations for the coefficients ϕ_k^{n+1} is derived:

$$a_{kj}^V \phi_j^{n+1} = c_k^n$$

where $a_{kj}^V = \int_0^1 M_k M_j d\sigma$ and c_k^n accounts for all known terms in (4) weighted with M_k . In order to comply with the bottom and surface boundary conditions, we took $M_k(\sigma) = \cos((k-1)\pi\sigma)$, $k \geq 1$, which are orthogonal functions in $L^2([0, 1])$ for which $a_{kj}^V = a_k \delta_{kj}$, so that the different vertical modes are uncoupled.

3.2.2 Horizontal discretization

A finite element method using bilinear quadrilateral isoparametric finite elements is employed for the 2D horizontal discretization. The solution is expanded as a linear combination of shape functions N_q attached to each nodal point, with the nodal values of the solution at time t_{n+1} and for vertical mode k as coefficients:

$$\phi_k^{n+1}(x, y) = \phi_{k,q}^{n+1} N_q(x, y)$$

Using again the Galerkin method of weighted residuals, a linear system for the nodal values is obtained, which can be written, for each $n \geq 0$ and $k \geq 1$, as:

$$a_{kk}^V b_{sq}^H (\phi_{k,q}^{n+1}) = c_{k,s}^n$$

where $b_{sq}^H = \int_{\mathcal{S}} N_s N_q d\mathcal{S}$. The advantage of using an explicit time advancement method is now clear since all the linear systems to be solved at each time step have the same system matrix, which is a mass matrix and is therefore symmetric, positive definite and sparse. Efficient numerical schemes for solving such systems are available and mass lumping can also be employed.

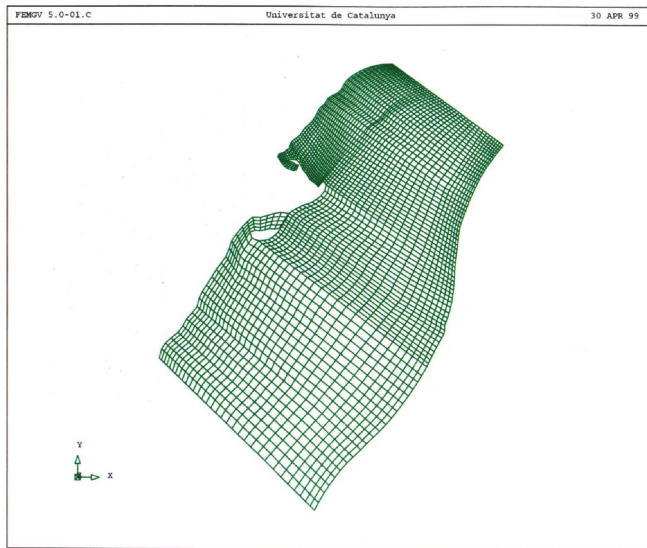


Figure 5.2 Ebro Delta Computational Mesh

Figure 1: The Ebro delta: computational mesh.

4 Applications

We present in this Section the application of the numerical scheme just described to the simulation of the dispersion of certain contaminants in two real-life situations: the dispersion of the plume of the Ebro river in the Mediterranean sea and the dispersion of the thermal outflow of some power plants in the Huelva estuary.

4.1 The Ebro delta

In this first case, we wanted to analyze the dispersion of contaminants at the mouth of the Ebro river concerning suspended matter of fine grain. This study was undertaken within the project FANS (Fluxes Across Narrow Shelves), which was financed by the European Union, intended to study the plume of the river from a hydrodynamical view point.

The two-dimensional finite element mesh used in this problem can be seen in Figure 1. It consists of 3004 quadrilateral elements and 3159 nodes, the average element size being $1\text{Km} \times 1\text{Km}$. A single vertical mode was used in this case. A homogeneous Neumann boundary condition was imposed everywhere except at the river mouth, where a known average concentration of 1.58 mg/l was given.

The velocity field for this problem was obtained numerically from a steady-state model (see [7]) under a typical Mestral wind (NW) situation, and it is shown in Figure 2. Once the mesh sizes and the velocities are known, stability

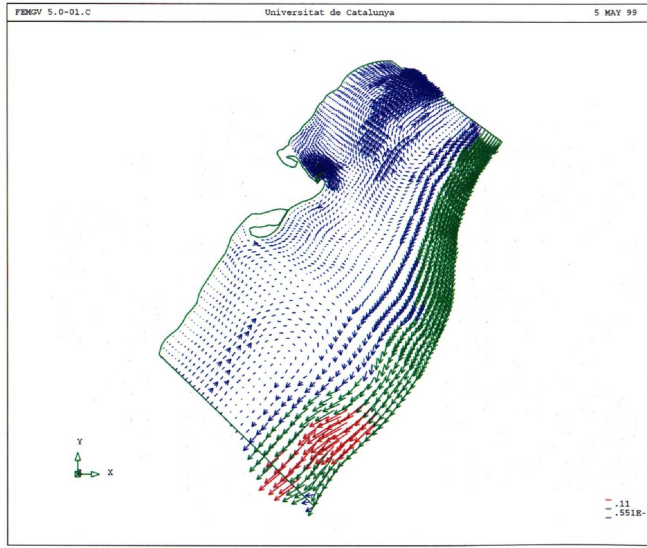


Figure 5.3 Velocity Field

Figure 2: The Ebro delta: velocity field.

restrictions for the time step size can be established. After some tests, a value of $\Delta t = 3$ min. was selected for this problem.

One of the difficulties encountered when solving real-life problems is that values or expressions for the model parameters are difficult to determine a priori. In this case, and in order to find the most realistic value of the horizontal diffusivity coefficient k_H , we performed a series of tests with four different values of this parameter: $k_H = 0.5, 1, 5$ and 10 , while the other parameters R and S were set to zero. The results obtained in each case at $t = 8$ hours can be seen in Figure 3. Taking into account both the overall appearance of the solution and its numerical values, a value of $k_H = 1$ was chosen.

Different values of the sedimentation velocity S were then compared: $S = 0, 10^{-5}, 10^{-4}$ and 10^{-3} . The best results seemed to be those for $S = 10^{-5}$ (see Figure 4), a value which we selected for the rest of the tests.

In order to check the stabilizing effect of the Characteristic-Galerkin formulation employed here, we solved the same problem with another model which uses a Taylor-Galerkin approximation (see [2]). The results obtained with this other method, which can be seen in Figure 5, show an unphysical behavior of the plume.

Finally, we present in Figure 6 the results obtained with the Characteristic-Galerkin method at different times: $t = 0, 15, 30$ and 45 hours, when a steady-state situation had already been reached.

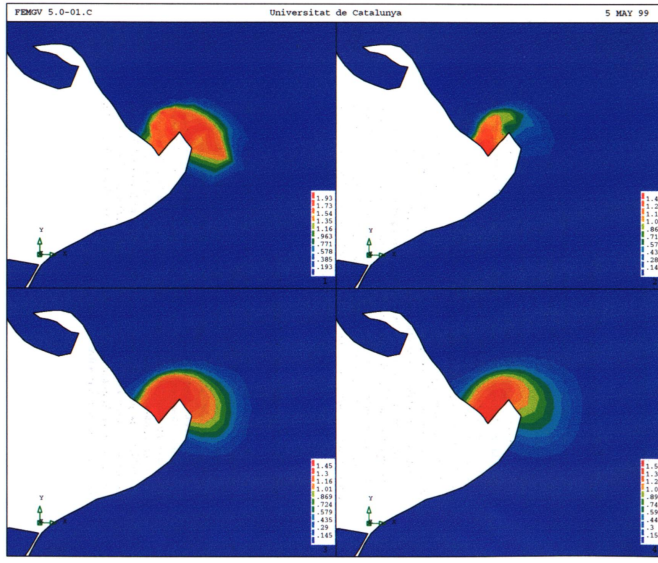


Figure 3: Results with $S = 0$ and: 1) $k_H = 0.5$; 2) $k_H = 1$; 3) $k_H = 5$; 4) $k_H = 10$.

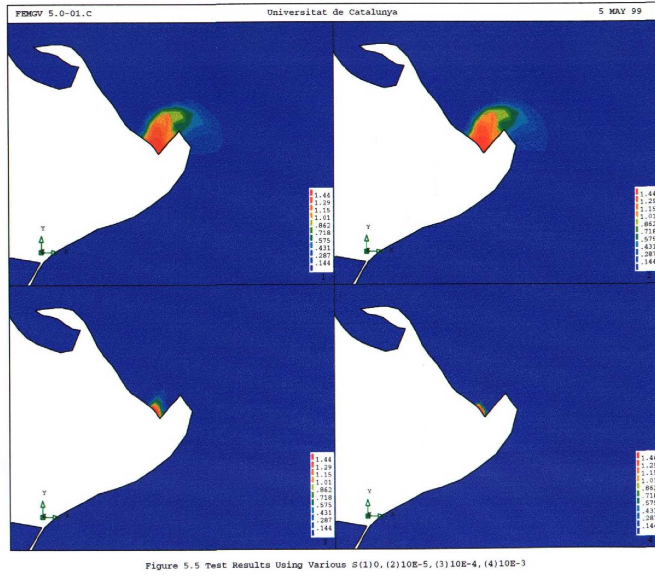


Figure 4: Results with $k_H = 1$ and: 1) $S = 0$; 2) $S = 10^{-5}$; 3) $S = 10^{-4}$; 4) $S = 10^{-3}$.

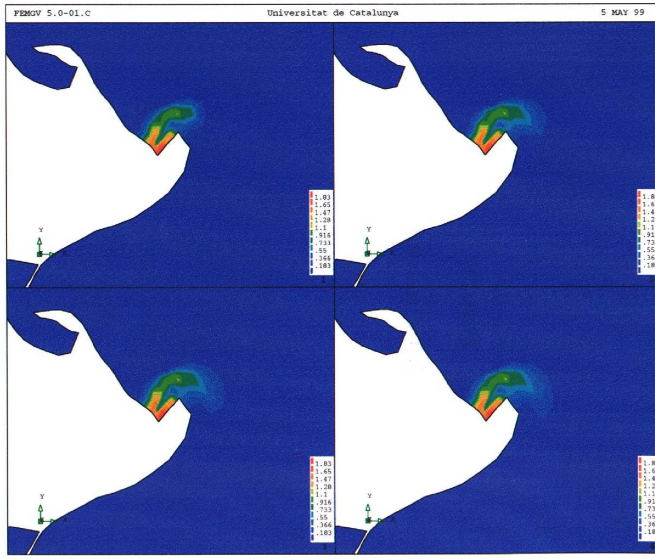


Figure 5.9 Test Results for RECODE with $Tf=80hrs$; $Ti=3mins$; $\alpha=10E-5$; $Kh=1$

Figure 5: Results with a Taylor-Galerkin model.

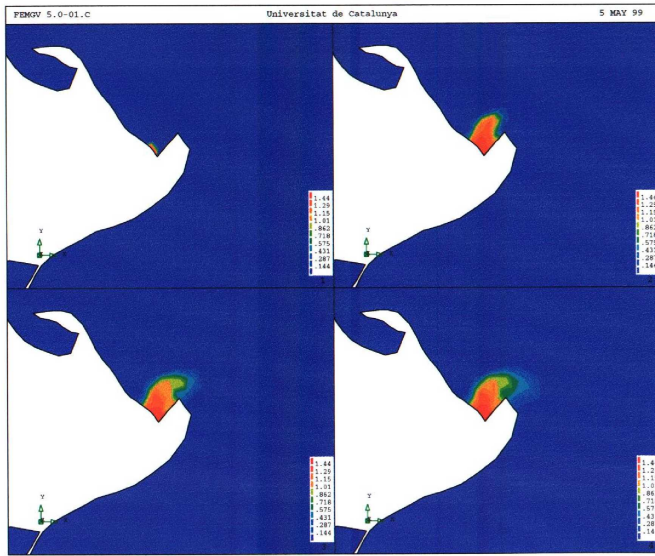


Figure 5.6 Dispersion of contaminants after (1) 0 (2) 15 (3) 30 (4) 45 hours

Figure 6: Results at: 1) $t = 0h$; 2) $t = 15h$; 3) $t = 30h$; 4) $t = 45h$.

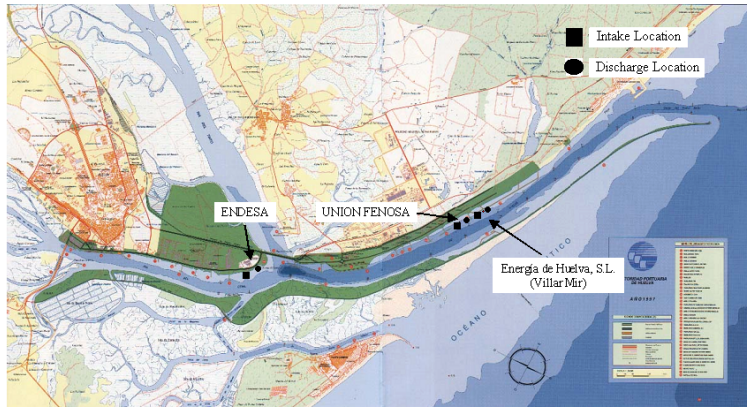


Figure 7: Location map of the Huelva estuary.

4.2 The Huelva estuary

In this second case we wanted to study the dispersion of the thermal outflow discharge of some power plants which might be constructed in the Huelva estuary on the Atlantic ocean, in the South-West of Spain. The Junta de Andalucía, the Andalusian regional government, has received the applications for the installation of three power plants in the area (see their location in Figure 7). The plant of Unión Fenosa would work with three groups or working units in its full capacity, the first one of which started operating in September 2004. In these plants, the water pumped from the river will serve as cooling agent and it will be discharged later as wastewater. We pretended to analyze the impact of this thermal outflow discharge in the temperature distribution in the estuary. This work was undertaken within a wider project of the Junta intended to study the overall environmental situation of the estuary.

Figure 8 shows the computational finite element mesh used, which has 3200 quadrilateral elements and 3531 nodes. The dimensions of the elements are

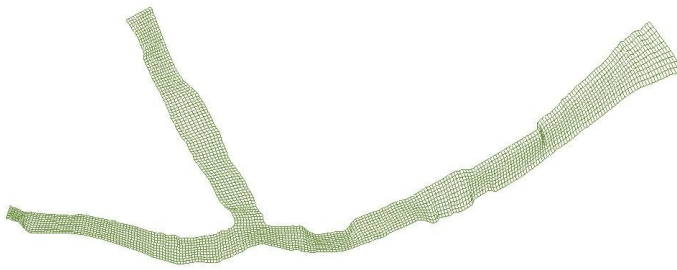


Figure 8: The Huelva estuary: computational mesh.

Plant	Unión Fenosa	Endesa	Energía de Huelva
Temperature ($^{\circ}\text{C}$)	6.6	6.5	9.0
Discharge (m^3/s)	0.338	0.338	6.67
Case 1	1	-	-
Case 2	2	-	-
Case 3	2	1	-
Case 4	2	-	1
Case 5	3	1	-
Case 6	3	-	1
Case 7	3	1	1

Table 1: Outflow discharge data and cases analyzed in the Huelva estuary

clearly irregular but the average element size is 100×100 meters. Homogeneous Neumann boundary conditions were imposed on all the boundary except at the discharge locations, where we used the discharge temperatures provided by the Junta.

The hydrodynamics in the estuary is mainly tidal. In order to obtain the velocity field and the free-surface elevations, the numerical model NAUTILUS was used for the mean flow while MAREAS provided the data for the numerical propagation of tides (see [4]). The values of the velocities, which are very irregular, range from 0 to 0.491 m/s ; Figure 9 illustrates an example of the non-steady velocity field.

In order to find the largest admissible value of the time step for this problem, we performed a series of test runs with increasing values of the coefficient of diffusivity k_H from 0 to the final value of $1 \text{ m}^2/\text{s}$, while the constant of transformation S was set to zero. As a result, the time step had to be limited to 15 seconds.

We then performed seven simulations with each case varying according to the number of power plants actively discharging wastewater and the number of working groups for each power plant (see Table 1). The results obtained after 15 days of simulation time can be seen in Figures 10 to 13 for four representative cases, where the temperature differences with the average temperature in the estuary are plotted. It can be observed (see Figure 11) how the effect of the plant of Unión Fenosa and that of Endesa discharging together (cases 3 and 5, the results for both of which were similar) increases the water temperature substantially, and that this increase is even larger when the plant of Energía de Huelva comes into operation (cases 4, 6 and 7, see Figures 12 and 13); as can be seen in Table 1, the proposed temperature jump and outlet discharge in this latter plant are higher than in the other two.

4.3 Conclusions

Various finite element methods can be used to solve transport equations. In this paper, we have presented the use of an explicit Characteristic-Galerkin method

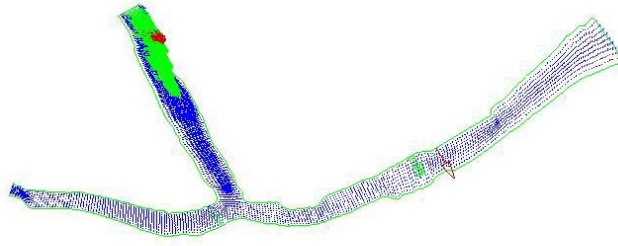


Figure 9: The Huelva estuary: an example of velocity field.

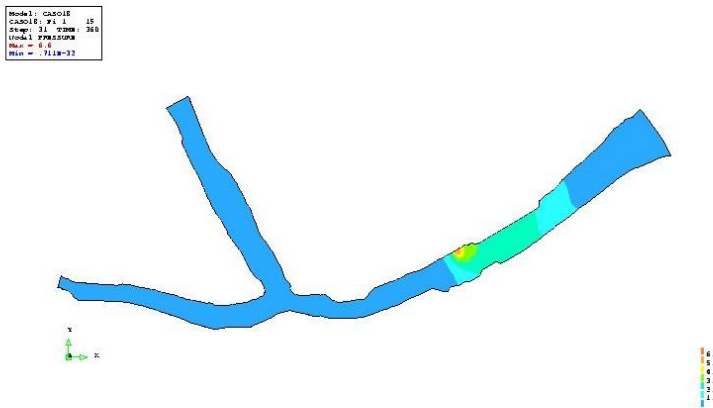


Figure 10: Results at $t = 15$ days for Case 1.

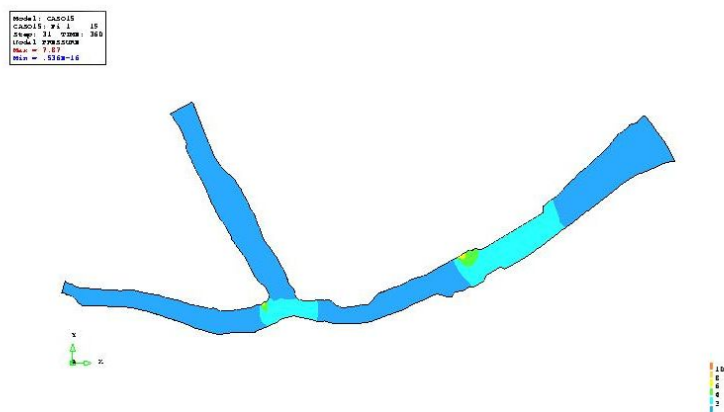


Figure 11: Results at $t = 15$ days for Case 3.

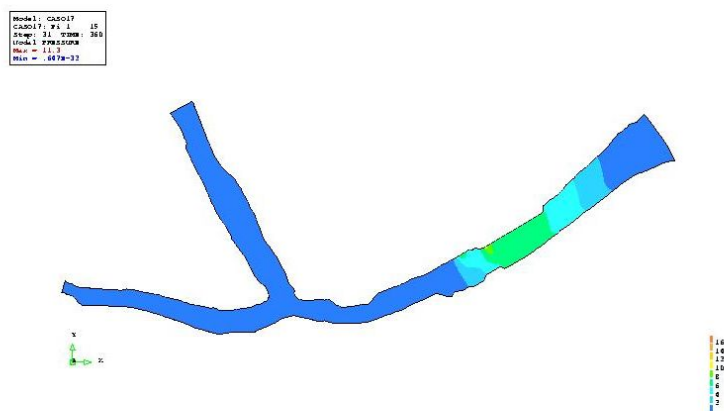


Figure 12: Results at $t = 15$ days for Case 4.

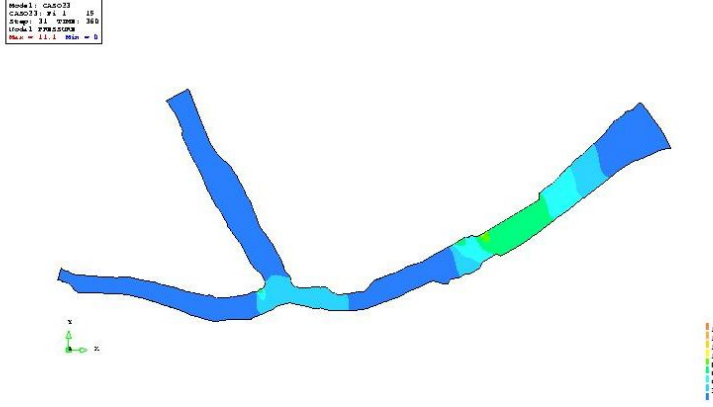


Figure 13: Results at $t = 15$ days for Case 7.

to develop a numerical model capable of simulating the dispersion of pollutants in a fluid medium. The model employs a quasi-3D spatial approximation, which results in a smaller computational cost than a fully 3D discretization. The numerical results obtained in the two applications considered are satisfactory, and indicate that the model provides a comprehensive tool to simulate contaminant dispersion.

In the case of the Huelva estuary, using the available parameters the simulation results show that when all three power plants are discharging water into the estuary, there is a notable change in water temperature. However, further calibration exercises must be done to verify the accuracy of some parameters with the help of real measurements which were not available during the time when the simulations were performed.

Acknowledgements

This work was partially funded by the Project *Profundización en el diagnóstico de la situación ambiental del Entorno de la Ría de Huelva*, of the Regional Government of Andalucía. The second author is under the auspices of the *Agencia Española de Cooperación Internacional*.

References

- [1] A.N. BROOKS, T.J.R. HUGHES *Streamline upwind Petrov–Galerkin formulations for convection dominated flows with particular emphasis on the incompressible Navier–Stokes equations*, Comp. Meth. Appl. Mech. and Eng., **32** (1982), 199–259.
- [2] J. DONEA *A Taylor-Galerkin method for convective transport problems*, Int. Jour. Num. Meth. Eng., **20** (1984), 101–119.
- [3] J. DOUGLAS, T.F. RUSSELL *Numerical Methods for convection dominated diffusion problems based on combining the method of characteristics with finite elements or finite differences procedures*, SIAM Jour. Num. Anal., **19** (1982), 871–885.
- [4] M. ESPINO, M.A. MAIDANA, A. SÁNCHEZ-ARCILLA, A. GERMAN *Hydrodynamics in the Huelva estuary. Tidal model calibration using field data*, Jour. of Waterway, Port, Coastal and Ocean Engineering, (2004), submitted.
- [5] T.J.R. HUGHES, L.P. FRANCA AND G. M. HULBERT *A new finite element formulation for computational fluid dynamics: VIII. The Galerkin/least squares method for advective–diffusive equations*, Comp. Meth. Appl. Mech. and Eng., **73** (1989), 173–189.
- [6] R. LEWIS *Dispersion in estuaries and coastal waters*, John Wiley and Son Ltd., Chichester 1997.
- [7] M.A. MAIDANA, J.J. NAUDIN, M. ESPINO, M.A. GARCÍA, A. SÁNCHEZ-ARCILLA *Feasibility and usefulness of diagnostic calculations of the mean circulation in the vicinity of the Ebro mouth. Model tests against field data*, Continental Shelf Research, **22** (2002), 229–245.
- [8] A. SÁNCHEZ-ARCILLA, M.A. GARCÍA *Selection of vertical profiles for quasi-3D modelling of shallow water circulation*, "Computational Methods in Surface Hydrology", G. Gambolati, A. Rinaldo, C.A. Brebbia, W.G. Gray and G.F. Pinder eds., 1990.
- [9] O.C. ZIENKIEWICZ, J.C. HEINRICH *A unified treatment of steady state shallow-water and two-dimensional Navier-Stokes equations - Finite element penalty function approach*, Comp. Meth. Appl. Mech. and Eng., **17-18** (1979), 673–698.
- [10] O.C. ZIENKIEWICZ, R.L. TAYLOR *The finite element method. Fifth Edition, Vol. 3*, Butterworth-Heinemann, London 2000.